PROPAGATION OF HYPERCONCENTRATED FLOWS IN PROTECTION CHANNELS AROUND URBAN AREAS: EXPERIMENTAL INVESTIGATION

Donatella TERMINI
Alice DI LEONARDO

INTRODUCTION

Recent catastrophic events due to intense rainfalls have mobilized large amount of sediments causing extensive damages in vast areas. These events have highlighted how debris-flows runout estimations are of crucial importance to delineate the potentially hazardous areas and make reliable assessment of the level of risk of urban areas.

Debris flow is a motion of a mixture of water, solid materials, rocks, etc. Thus, according with Rickemann (1999), debris flows could be considered as a phenomenon intermediate between landslides or rockfalls and fluvial sediment transport. The occurrence of debris flow is not easily predictable. One of the main uncertainties of the existing runout estimation methods is related to the need of knowing input parameters that can be difficult to estimate (Rickemann, 1999; Prochaska et al., 2008).

Especially in recent years, several researches have been conducted in the attempt to define estimating methods of the most important parameters of debris-flow behavior. Experimental works as well as numerical simulations (among others Natarajan et al., 1995; Louge & Keast, 2001; Pudasaini et al., 2005; Armanini et al., 2009) have also allowed the assessment of the physics of the debris flows. The major part of the experimental studies has especially analyzed the rheological characteristics of the debris flow and the basic kinematic conditions which determine the phenomenon evolution (see as an example Armanini et al., 2005). Furthermore, due to the complexity of the debris-flow process, numerical simulation models of debris flows are still limited. The point is that the design of protective measures requires the knowledge of the propagation conditions (Mizuyama, 2008).

In recent years, several debris flow phenomena have occurred in different areas of Italy. In the present work, attention is especially devoted to the event of October 2009 occurred in Sicily (Italy). Intense precipitation event caused loss of lives and great damages to infrastructures and housing, especially in Giampilieri, that is a small urban area included in the territory of Messina. After this event, in the ambit of activities of reconstruction and protection of the urban area, the Regional Authority decided to design a conveyor channel enclosing the urban area of Giampilieri in order to prevent (or to limit) future damages. Analysis of the performance of the conveyor channel in a laboratory physical model was assigned to University of Palermo.

The present work addresses the issue of the experimental analysis of the effect of a defence channel on the flow propagation, with particular reference to the designed conveyor channel in Giampilieri's urban area. To this aim, eexperimental program has been recently conducted at the Hydraulic laboratory of the Department of Civil, Environmental, Aerospatial and of Materials Engineering (DICAM) – University of Palermo (Italy). The experiments were carried out in a flume appositely constructed and were planned in order to analyze the influence of the geometrical characteristics of the inflow confluences on the

propagation phenomenon. In this paper, preliminary results of the analysis concerning peculiar factors (such as the slope and the bed roughness) characterizing the inflow channel (hereafter called as "inflow confluence") at the confluence section of the conveyor channel are reported.

EXPERIMENTAL INSTALLATION

The experimental apparatus is shown in Figure 1 (Figure 1a reports the render and Figure 1b reports the plane view). The apparatus is composed of two main parts: the main channel, in which the flow is conveyed until the reaching of the downstream tank (Figure 1a), and the so-called distribution channel, which is connected to the main channel through three inflow confluences (indicated in Figure 1b with the abbreviations "InR1", "InR2", "InR3"). The main channel is 5.7 m long. The cross-section is rectangular with width of 22 cm along the reach between section 1 (see Figure 1b) and the section downstream of the inflow confluence InR3; the width is of 17.5 cm in the remaining part of the channel. The channel bed is of concrete with constant longitudinal slope of 15%; through a movable system it is possible to vary the bed slope of ±5%. The side-walls are of Plexiglas strips 26 cm high. The distribution channel is composed by three sub-channels; each sub-channel is connected to the upstream end of the corresponding inflow confluence through a small hopper. Three slice gates, located at the bottom of the upstream tank (see Figure 1) allow the activation and regulation of the discharge in each inflow confluence, InR. The upstream tank is located at the upstream end of the distribution channel, as shown in Figure 1.

During the experimental runs, the fluid entered on the upstream tank through the recirculating pumping system which includes a PEAD pipe (Φ 100 mm), two regulation valves and a submerged pump inside the downstream tank located at the downstream end of the main channel (see Figure 1).

Several runs were conducted varying the volume discharge, the sediment concentration and the geometrical configuration of the inflow confluences. In the present work attention is restricted to inflow confluence InR1. For this reason, the experimental runs considered in the following analyses have been performed by closing the slice gates upstream of the InR2 and InR3 confluences.

Under the aforementioned conditions, two series of runs were conducted for different values of the volume discharge. The first series of runs (hereafter denoted as "series I") was carried out with clear water (hereafter denoted with abbreviation CW) while the second series of runs (hereafter denoted as "series II") was performed with a mixture (hereafter denoted with abbreviation "MR") of water and sediment material and for different values of the sediment concentration. The sediment material used in series II runs was taken from the area of the debris flow occurred in Giampilieri on October 1, 2009. During each run, the water depths were continuously measured both by two radar probes (Sitrans Probe LR radar pulse technology at 5.8 GHz) and by four pressure transducers. The measures were performed at reaching of the stationary conditions. The radar probes and the pressure transducers were located at the axis of peculiar sections opportunely selected along the channel. The pressure transducers were based on Wheatstone bridge and were connected to a small pipe located at the bottom of the channel. The radar probes were supported by a carriage on the channel's side-walls, so as these probes could be moved along the channel. The position of the pressure transducers and of the radars can be visualized in Figure 1b. Furthermore, dur-

ing each run, the longitudinal profiles of the free surface visible at the right bank were continuously recorded by a high-resolution video-camera Panasonic 3CCD (1.7 Megapixel).
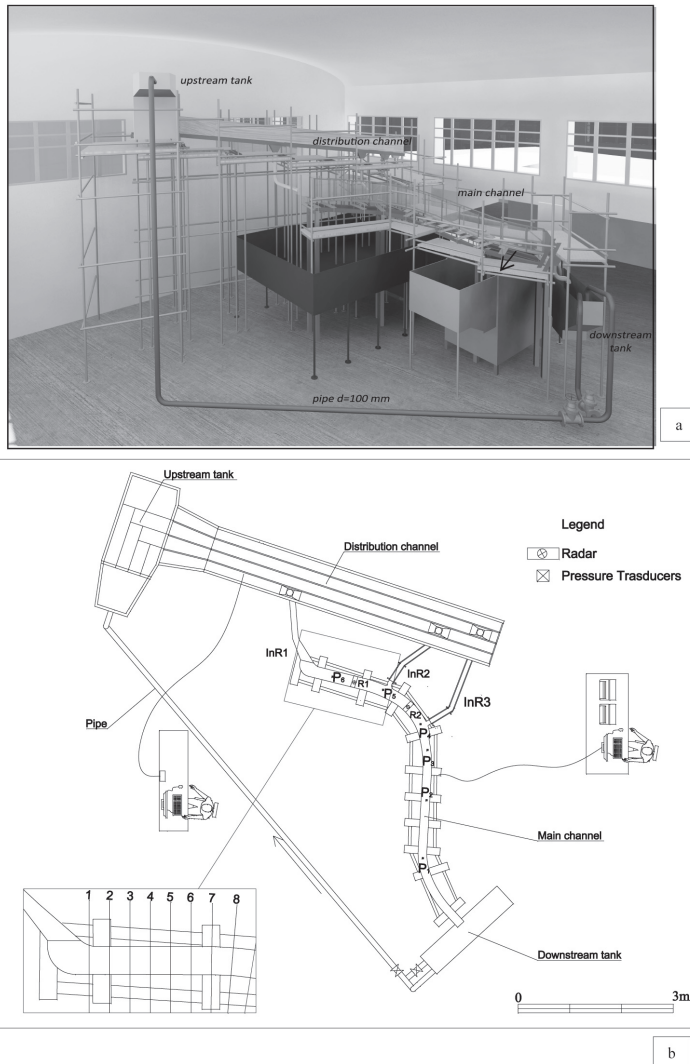

Fig. 1: Experimental Apparatus: a) Render; b) Plane-view

METHODS AND EXPERIMENTAL RESULTS
Methods

The investigation aimed at verifying how the geometric configuration and the bed roughness of the inflow confluence InR1 (see Figure 1) affect the flow pattern along the conveyor channel. This is important to verify the performance of the conveyor channel at different stages of the propagation phenomenon. To this aim, first, in order to identify the

best performing configuration, the runs of series I-CW were conducted; then, once the best performing configuration was chosen, the fluid mixture behaviour along the channel was examined during the runs of series II-MR.
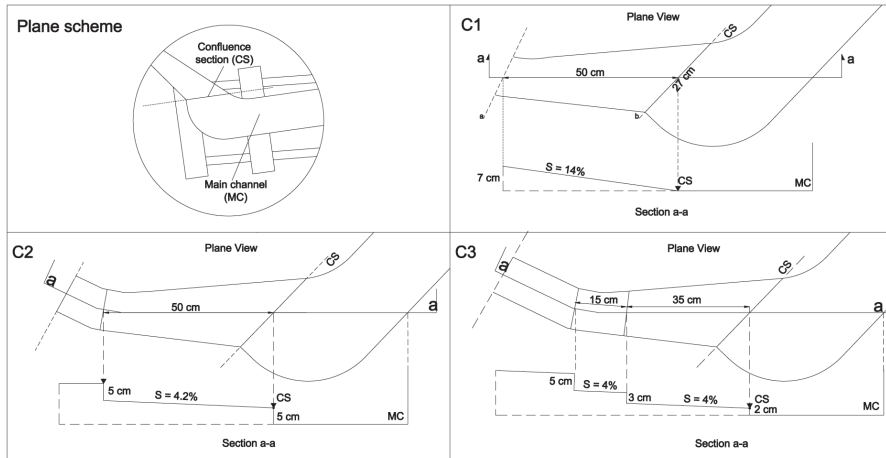
Three geometrical configurations and four macro-roughness conditions were investigated. Figure 2 reports the plane-views and the longitudinal sections of the tested configurations. In particular, the following geometrical variations of the inflow confluence InR1 were tested (see Figure 2a): C1, which is characterized by a uniform longitudinal slope of 14 % until the reaching of the confluence section (i.e. the section at the downstream end of inflow confluence - hereafter the confluence section is indicated with abbreviation "CS"); C2, which differs from configuration C1 because of a lower longitudinal bed slope (slope of around 4%) and because of the presence of two jumps (height of 5 cm) respectively at the confluence section and at the section upstream of the InR1 reach; C3, which is characterized by bed slope almost equal to that of configuration C2 and by the presence of three jumps (one of height of 3 cm at the confluence section, another one of height of 5 cm at the section upstream of the InR1 reach and another one, of height of 2 cm, at an intermediate section).

The analysis of the effect due to the presence of macro-roughness elements on the bed has been performed by considering both the case of elements with irregular geometry and shape (such as the stones) and the case of elements of regular geometry. In the first case, pebbles were glued on the bed of the inflow confluence; in the second case wooden squared parallelepipeds (of horizontal area of 1 cm^2) were used. In the last case, two conditions were examined: 1) high parallelepipeds (height of 6 cm); 2) short parallelepipeds (height of 3 cm). The macro-roughness elements were distributed in an alternating way along the InR1 confluence. Figure 2b shows the plane scheme of the distribution of the macro-roughness elements and the longitudinal sections of each type of examined configuration (Type 1, Type 2, Type 3, and Type 4 of Figure 2b). It can be seen from this figure that each configuration is determined by a peculiar combination of a specific geometrical configuration (as reported in Figure 2a) and a specific macro-roughness distribution.
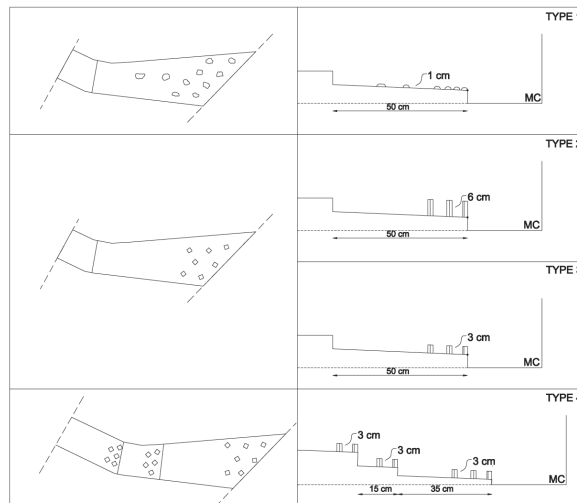
Table 1 reports the series of runs performed and the corresponding geometrical configuration and volume discharge, Q.

	Run	Q	configuration/Type
		l/s	
Series I,a	CW1	2,18	C1
	CW2	3,29	C1
	CW3	3,31	C1
	CW4	4,66	C1
Series I,b	CW5	3,97	C2
	CW6	3,91	C3
Series I,c	CW7	3,31	C2, TYPE 1
	CW8	3,90	C2, TYPE 2
	CW9	3,61	C2, TYPE 3
	CW10	4,64	C3, TYPE 4
Series II	MR1	3,21	C3, TYPE 4
	MR2	4,96	C3, TYPE 4
	MR3	4,96	C3, TYPE 4

Table 1: Characteristics of the Experimental Runs

Fig. 2: Investigated Configurations: a) geometrical variations; b) plane-view and longitudinal section of macro-roughness combination types

As Table 1 shows, series I includes three groups of runs: runs CW1-CW4 (i.e. "series I,a"), which have been performed in order to examine the flow behavior, by using the simplest geometrical configuration C1, for increasing values of the discharge Q; runs CW5-CW6 (i.e. "series I,b") performed in order to compare the flow behavior between different geometrical configurations (i.e. configurations C1, C2, C3) for an almost constant value of the volume discharge; runs CW7-CW10 (i.e. "series I,c") performed in order to analyze the flow behavior between different macro-roughness combinations, for almost constant volume discharge and by using the same geometrical configuration. The series II includes three

runs (MR1, MR2 and MR3) performed by using the geometrical configuration selected on the basis of the results obtained during runs of series I, but varying the discharge and the sediment concentration.

Experimental results
-Series I:

Figure 3 reports the longitudinal profiles of the free surface measured at the right bank of the channel during runs of series I. First, in order to analyze the performance of the configuration C1 for different values of volume discharge, the series I,a have been carried out. The longitudinal profiles of the free surface measured during the runs of series I,a are compared in Figure 3a. This figure shows that all the profiles have an increasing trend between section 1 and section 3; close to section 3 the profiles assume a peak value and then they have a decreasing trend. This behaviour could be related to the fact that at the confluence exit, the fluid jet is characterized by high velocity and kinetic energy. This energy is then dissipated by bumping into the right bank of the channel. As the volume discharge increases (CW3 and CW4 runs), the flow depths increase too so as to determine the risk of the bank overflowing.

An attempt to limit the aforementioned risk was made by adding either two jumps (configuration C2 – run CW5) or three jumps (configuration C3 - run CW6). Figure 3b shows the comparison between the longitudinal profiles measured during series I,b and the profile obtained during CW3 run (that was carried out by using the configuration C1 and for a value of volume discharge close to that used during CW5 and CW6 runs). From Figure 3b it appears clear that the presence of jumps does not reduce the risk of the bank overflowing. Among the geometrical configurations examined, C2 seems to have the best performing behaviour. In fact, when C2 is used lower values of the flow depths at the right bank are obtained. Furthermore, the length of the channel reach interested by the risk of bank overflowing is shorter than that observed with configurations C1 and C3.

Then, the effect related to the presence of macro-roughness elements on flow pattern has been investigated during series I,c runs (see Table 1). In particular, by considering the macro-roughness types of Figure 2b, the following tests have been performed: I) by using the best performing configuration C2 (obtained as result of runs of series I,b) and varying the typology of the macro-roughness elements (i.e., in particular, with irregular-shaped elements type 1 -run CW7-, with regular-shaped high parallelepipeds type 2 -run CW8-, with regular-shaped short parallelepipeds type 3 -run CW9- (see Figure 2b and Table 1); II) by using a new combination of three jumps (i.e. configuration C3) and the best performing macro-elements chosen as result of test I (i.e. type 4 of Figure 2b). The comparison of the longitudinal profiles measured at the right bank during CW7-CW9 runs (test I) is reported in Figure 3c. This figure shows that after the introduction of the macro-roughness elements, the peaks of the profiles decrease in value avoiding the risk of the bank overflowing. Furthermore, it can be seen that in CW9 run the peak values occur along a channel reach shorter than that observed in CW7 and CW8 runs. This means that the short regular-shaped elements represent the best performing macro-roughness typology. Thus, the short regular-shaped elements have been used for test 2 and the combination type 4 of Figure 2b has been investigated (CW10 run). The comparison between the longitudinal profiles measured during CW9 and CW10 runs are reported in Figure 3d. It should be noted that (see also Table

1) CW10 has been conducted with volume discharge higher than that used for CW9. It can be observed from Figure 3d that the peaks of the longitudinal profiles reduce strongly in value when the combination type 4 is used, even with high values of volume discharge. Furthermore, on the contrary of that observed for CW9 run, the longitudinal profile measured during CW10 run assumes a gradual decreasing trend after section 2. The behaviour observed by using the combination type 4 is probably related to the presence of the jump at the upstream end of the inflow confluence, which allows the flow kinetic energy could be partially dissipated before to reach the confluence section.

-*Series II*:

This series of runs have been performed in order to analyze how/if the addiction of sediment material influences the flow pattern observed during runs of series I. To this aim, the best performing combination (type 4), obtained as result of series I runs, has been used. The runs of series II were performed for increasing values of volume discharge and sediment concentration. For the analysis presented in this work, the sediment concentration was around of 4% in MR1, around of 3% in MR2 and around of 6% in MR3. Figure 4 reports the comparison between the longitudinal profiles measured during runs MR1, MR2 and MR3. This figure shows that the profiles assume a gradual decreasing trend until to reach section 8, as well as observed in CW10 run, with a peak value slightly lower than that obtained in CW10 run. Furthermore no peculiar differences between the profiles determined for different sediment concentrations have been observed. This means that for the sediment concentrations investigated, the addiction of sediment material does not determine significant changes on the flow pattern.
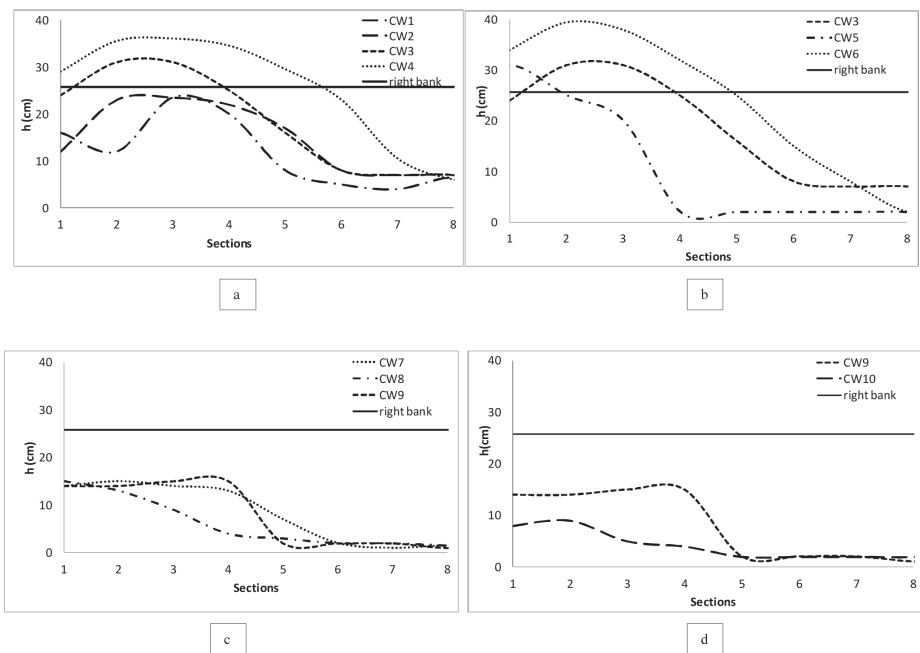

Fig. 3: Comparison between Measured Profiles of the free Surface: a) series I,a; b) series I,b; c) series I,c; d) series I,d;
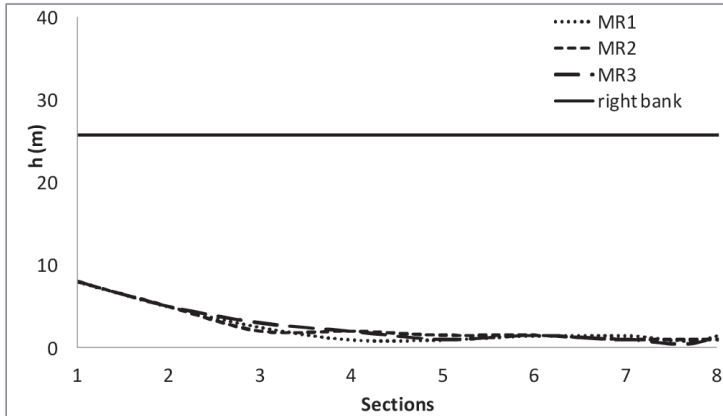
Fig. 4: Comparison between Measured Profiles of the Free Surface – series II

CONCLUSION

The present paper reports preliminary results of experimental investigation on the effect of defence structures on debris flow propagation. In particular, the investigation was conducted in a laboratory flume which follows the conveyor channel under construction in Giampilieri (Sicily- Italy). In this work, the analysis concerns the influence of the geometrical characteristics of the inflow confluence on the flow pattern along the conveyor channel and, consequently, the performance of the channel itself in regards to the bank overflowing risk. Different configurations of the inflow confluence have been tested. These configurations have been selected in order to investigate: a) the effect due to the variation of the longitudinal bed slope; b) the effect due to the addiction of jumps; c) the effect due to the addiction of macro-roughness (both of irregular and regular geometry) elements on the bed; d) the effect of the addiction of sediment material with increasing concentration. The results have shown that the best performing configuration is given by the combination of jumps and macro-roughness elements, opportunely distributed along the inflow confluence reach. In fact, it has been observed that by using such a combination the high kinetic energy of flow at the confluence section is already partially dissipated upstream of this section because of the presence of the jumps; the macro-roughness elements, distributed alternating along the inflow reach, allows to enlarge the flow cross-section and to further dissipate the flow energy. Furthermore, for the sediment concentrations investigated, the addiction of sediment material does not determine significant changes on the flow pattern.

REFERENCES

ARMANINI A., CAPART H., FRACCAROLLO L., LARCHER M., (2005). Rheological stratification in experimental free-surface flows of granular-liquid mixtures. Journal Fluid Mechanics, vol. 532, 296-319.

ARMANINI A., FRACCAROLLO L., ROSATTI G., (2009). Two-dimensional simulation of debris flows in erodible channels. Computers & Geosciences, vol. 35, 993-1006.

LOUNGE M.Y., KEAST S. (2001). On dense granular flows down flat frictional inclines. Physics of Fluids. 13(5), 1213-1233.

MIZUYAMA T. (2008). Structural Countermeasures for Debris Flow Disasters. International Journal of Erosion Control Engineering, 1(2), 38-43.

NATARAJAN V.V.R., HUNT M.L., TAYLOR E.D. (1995). Local measurements of velocity fluctuations and diffusion coefficients for a granular material flow. Journal Fluid Mechanics, vol. 304, 1-25.

PUDASAINI S. P., WANG Y., HUTTER K. (2005). Modeling debris flows down general channels Natural Hazards and Earth System Sciences, vol. 5, 799–819.

PROCHASKA A. B., SANTI P.M., HIGGINS J.D., CANNON S.H. (2008). Debris-flow runout predictions based on the average channel slope (ACS). Engineering Geology, vol. 98, 29–40

RICKENMANN D., (1999). Empirical Relationships for Debris Flows. Natural Hazards. vol. 19, 47–77.